STATE RESEARCH CENTER OF RUSSIA
INSTITUTE FOR HIGH ENERGY PHYSICS

IHEP 2007-22

V. Ammosov, V. Gapienko, A. Ivanilov, A. Semak, Yu. Sviridov, V. Zaets

(Institute for High Energy Physics, Protvino, Russia)

E. Usenko

(Institute for Nuclear Research, Moscow, Russia)

Study of RPCs with 1×1 cm^2 Read-Out Pads Operated in the Saturated Avalanche Mode

Protvino 2007

UDK 537.5 M–24

Abstract

Ammosov V., Gapienko V., Ivanilov A., SemakA., Sviridov Yu.*), Zaets V., Usenko E. Study of RPCs with 1×1 cm^2 Read-Out Pads Operated in the Saturated Avalanche Mode: IHEP Preprint 2007-22. – Protvino, 2007. – p. 15, figs. 11, tables 1, refs.: 6.

Monogap glass Resistive Plate Chamber (RPC) prototypes equipped with 1×1 cm^2 read-out pads and operated in saturated avalanche mode were studied as a possible detector for a digital calorimetry. Operating characteristics of the prototypes such as induced charges, efficiencies and fired pad multiplicities as a functions of applied voltage were measured for different gas mixtures, gas gap widths, anode thickness, electronics thresholds and beam incidence angles.

Key words: glass RPC, saturated avalanche mode, digital read-out.

PACS 29.40.Cs.

Аннотация

Аммосов В.В., Гапиенко В.А., Заец В.Г., Иванилов А.А., Свиридов Ю.М.*), Семак А.А., Усенко Е. Изучение резистивных плоских камер с сигнальными элементами размером 1×1 см^2 в режиме насыщенной лавины: Препринт ИФВЭ 2007-22. – Протвино, 2007. – 15 с., 11 рис., 1 табл., библиогр.: 6.

Исследованы прототипы однозазорных резистивных плоских камер (РПК) как возможных детекторов для цифровой калориметрии. Прототипы имели стеклянные резистивные электроды, были оборудованы сигнальными элементами 1×1 см^2 и работали в режиме насыщенной лавины. Измерены рабочие характеристики РПК, такие как индуцированные заряды, эффективности и множественности сработавших падов в зависимости от приложенного напряжения для нескольких газовых смесей, разных ширин газового зазора, толщин резистивного анода, порогов электроники и углов падения пучка.

Ключевые слова: стеклянные резистивные плоские камеры, режим насыщенной лавины, цифровое считывание.

*) Corresponding author, E-mail: Yuri.Sviridov@ihep.ru

1 Introduction

Employment of the Resistive Plate Chambers (RPC) with highly segmented read-out electrodes as the active detector for the digital hadron calorimeter (DHCAL) at future linear e^+e^--collider such as ILC was proposed several years ago (see, for example, [1]). The requirements to DHCAL and RPCs based on the considerations of physical tasks were formulated in [2, 3].

The main requirements to an RPC are as follows:

– it should be thin to fit into about 6 mm free space between DHCAL absorbers;

– should have small read-out pads of 1×1 cm^2 dimensions;

– should have high ($\simeq 98\%$) efficiency for charged particles;

– should have low (≤ 1.5) multiplicity, that is, number of pads fired per one throughgoing particle [3].

Studies of these and other items were performed with small prototypes. The prototypes operated in the saturated avalanche mode. In this paper we present the results of this work. The characteristics, essential to evaluate the possible use of such RPC in the DHCAL, such as efficiency and fired pad multiplicity were measured for several gas mixtures and electronics thresholds. The steps to optimize the prototype design in order to reduce the multiplicity were done.

This work was done in the framework of the ECFA/DESY study for a future electron-positron linear collider [4] which calorimetric aspects are treated in a world collaboration called CALICE [5].

2 Prototype design and experimental set-up

Essentially, an RPC is a gaseous detector representing a stack of two resistive electrodes placed parallel to each other at some distance (gas gap) provided by spacers. High voltage is applied to the outer surfaces of the resistive electrodes by means of conductive substance thus creating strong electric field inside gas gap. Charged particle produces ionization in gas gap. Due to high electric field electron avalanche is developed. High resistivity of electrodes ensures

localisation of an avalanche and prevents detector from breakdown. Read-out electrodes placed on both sides of the stack detect current pulses induced by avalanche developement.

In our prototypes, the resistive electrodes were made of commercially available glass. Glass was chosen due to its higher surface quality as compared to bakelite and hence lower intrinsic noise level. The resistivity of glass was about 7×10^{12} Ω·cm. As thin as possible (and accessible at the moment) glass sheets were used. The cathode glass plate was 1 mm thick and the anode one 0.67 mm thick. The gaps between glass plates were provided by the PVC buttons of 6 mm diameter glued to the glass electrodes on about (4×4) cm lattice. Small size of the lattice was required due to rather thin glass plates and strong electrostatic forces between electrodes. In order to optimize the RPC performance while keeping the overall detector thickness small, several gaps of different width d were tested, namely, 0.8, 1.2, 1.6 and 2.0 mm.

Self-adhesive graphite films of 0.12 mm thickness were glued to the outer surfaces of the cathodes of all prototypes to provide the applied voltage distribution. The surface resistivity of these films was measured to be about 10 MΩ/square. Normally the source of negative voltage was used so the cathode had high potential up to 12 kV for the 2 mm wide gas gap. The 0.2 mm thick mylar films were glued to the cathodes in all prototypes for insulation. Cathode readout pad of about (7×7) cm^2 was attached to this film to provide the charge measurements.

From the anode side normally also the same graphite film was glued to the anode glass electrode and the mylar insulator was 0.05 mm thick.

The 16 anode pads of (1×1) cm^2 dimensions were made on the 1.5 mm thick G10 printed circuit boards forming (4×4) matrix with 0.5 mm distance between pad edges.

The gas gaps with attached read-out electrodes were inserted in the gas tight aluminum boxes. A few soft rubber pieces between the upper read-out electrode and outer cover of the boxes provide nesessary compressing of read-out electrodes to the gas gap stack. The overall thickness of prototypes does not exceed the required 6 mm limit.

Two gas mixtures of $C_2H_2F_4/iC_4H_{10}/SF_6$, namely 93/5/2 and 90/5/5 in the flow rate composition, were tested.

The prototypes were installed in the 5 GeV/c positive hadrons beam. The beam width was about 4 cm FWHM. Five scintillation counters defined (2×2) cm^2 trigger area covering four central pads.

The output signal of the cathode pad was inverted, amplified by 10 and sent to the QDC unit with 0.25 pC least count for the charge measurements. Signals from sixteen anode pads were fed through the walls of the box by twisted pairs about 10 cm long to the external LEMO-type connectors and then connected by 40 cm long coaxial cables to the 16 channel ATL16 amplifier-discriminator [6], output ECL signals of which were sent to the TDC and used for the efficiency and multiplicity measurements. Charge was measured in 150 ns wide gate and the time window for TDC was 350 ns wide.

Four threshold values, 0.6; 2.2; 5.0 and 10 mV at the ATL16 inputs, were tested in order to find optimal operating point and to define the requirements for the front–end electronics development.

3 Experimental results

In Figures 1 to 3 the behaviour of efficiency, multiplicity and mean charge in dependence on the applied voltage is shown for the prototypes with 1.2; 1.6 and 2 mm wide gaps, respectively. Data for the both mixtures are presented.

All these prototypes showed high efficiency (more than 98%) for all thresholds and both gas mixtures. The exception is 1.2 mm prototype at 5 mV threshold; it reaches only 96% efficiency.

Mean charges Q increase exponentially up to about 6 pC in operating regions for all protypes shown. The shapes of the charge distributions are typical for the saturated avalanche mode. Relative width of the distributions that is the ratio of the RMS deviation of the charge distribution to its mean value is higher for the more narrow gaps. Typical values of the relative width were about 0.7 for the 1.6 mm wide gap and 1.2 for the 0.8 mm wide one in the operating point (mean charge about 4 pC).

The mean multiplicity M also increases with the applied voltage. Increasing threshold from 0.6 to 2.2 mV reduces multiplicity significantly without loss of efficiency. For higher thresholds the effect of multiplicity reduction becomes weaker and the efficiency is decreased.

Fig. 4 presents as an example the data on correlation between the efficiency ε and mean multiplicity M for the prototype with 1.2 mm gap at several thresholds and for both gas mixtures. It is seen from Fig. 4-a that, for instance, at the efficiency of 96% the multiplicity is 1.3; 1.35 and 1.5 for thresholds 5.0; 2.2 and 0.6 mV, respectively. On the other hand there is no difference in this correlation between two mixtures.

In Fig. 5 such a correlation is shown for the prototypes with gap width 1.2; 1.6 and 2.0 mm at 2.2 mV threshold. For all prototypes, efficiency of 98% is achieved at M = (1.3 – 1.35). No systematical difference in (ε vs M) — correlation curves for prototypes with different gap width is seen within our accuracy. Thus, in these most important characteristics, all gas gaps in the range 1.2–2.0 mm are identical.

In Fig. 6 we show the dependence of efficiency on the mean charge for prototypes with gap width 2.0; 1.6; 1.2 and 0.8 mm at two thresholds and for both gas mixtures. Again there is not seen significant difference between prototypes with 1.2; 1.6 and 2.0 mm wide gaps. For all of them threshold mean charge (that is charge at which the efficiency is 50%) is about (100±20) fC at 0.6 mV voltage threshold and about 300–400 fC — for the 2.2 mV one. The efficiency plateau is achieved at $\simeq$(1–2) pC and $\simeq$(3–4) pC, respectively. For the more wide gaps the plateau starts at slightly lower mean charges.

It is seen also that the prototype with 0.8 mm gap reaches only 90–92% efficiency for the 0.6 mV threshold and 87% at the 2.2 mV one. It seems that these thresholds are not low enough for this gas gap due to considerably wider charge distribution in comparison with other gaps as it was said above.

Obviously the prototypes with different gap width have different HV operating regions as it is shown in Fig. 7a. These figure show the voltage value V_{knee} for 98% efficiency for prototypes with gap widths 1.2, 1.6 and 2.0 mm for 2.2 mV threshold and both gas mixtures. It is seen that the operating HV increases on 0.8 kV for every 0.4 mm step in gas gap width for the mixture with 2% of SF_6 and on about 1.3 kV for the 5% of SF_6 mixture.

As it is seen from Figures 1(a,b) to 3(a,b), the efficiency curves in dependence on applied voltage start to drop at some critical HV values in all cases. This is probably due to high resistivity of the glass, increased noise rate and increased fraction of the large avalanches or streamers. Therefore the width of the operating region can be determined as a HV interval ΔV in which the efficiency is higher than the required value of 98%. This width depends on the threshold and on the gap width. It does not depend on the SF_6 fraction in gas mixture within about (100–200) V uncertainty.

The dependence of ΔV on the threshold for three prototypes with 1.2; 1.6 and 2.0 gap width is shown in Fig. 7b; the data for two mixtures are avereged. It is seen from Fig. 7b that the width of the operating region is almost the same for all three prototypes at the lowest threshold 0.6 mV. For higher thresholds ΔV is equal for the 1.6 and 2.0 mm prototypes and significantly shorter for the 1.2 mm one. There is practically no plateau for this prototype at 5 mV threshold.

At 10 mV threshold only scarce measurements were done due to low efficiency for all prototypes as it is clear from Fig. 7b.

The drop in efficiency is accompanied by the slowing-down of the mean charge growth in dependence on HV, see Fig's 2f and 3e. For even higher HV, the mean charges start to decrease.

Significant difference was observed for the prototypes with different gap width in the intrinsic noise level. In Fig. 8 the noise rates for counters with 1.2; 1.6 and 2.0 mm wide gaps at two threshold values are shown as a function of electrical field strength E; SF_6 concentration was 5%. The arrows on this figure depict the plateau knee values of E. The noise rate in operating region is systematically lower for the wider gaps.

For imaging calorimetery it is desirable to further decrease the hit multiplicity in order to have, ideally, one fired pad per one through going particle. One way in this direction was outlined in our initial studies of similar RPCs in the streamer mode [2]. It was found that the pads multiplicity can be reduced significantly by using more thin resistive anodes. Here we carried out more systematical study of this effect by changing the anode insulator thickness in the 1.2 mm gap prototype to simulate the increase of the anode thickness t_A.

The results are shown in Fig. 9. These data were obtained at the 2.2 mV threshold. Numerically, for 3 pC mean charge (the plateau knee at this threshold, see Fig. 6) the multiplicity M $\simeq$ 1.22 if there is completely no additional material on the anode glass and the readout panel is pressed directly to the glass outer surface (t_A = 0.67 mm). On the other hand M = 1.6 for the case when the graphite film and 0.45 mm thick mylar insulator are placed between the anode glass and the pads panel ($t_A \simeq$ 1.24 mm). These results confirm our previous observation. The practical way to use this possibility of reducing hit multiplicity still has to be found.

For some FEE schemes positive input signals will be preferable. We verified this variant of the RPC read-out by inverting the applied HV and using ATL161 modification of the amplifier — discriminator which was suited for positive input signals. Comparison of the multiplicity dependence on induced charges for the both cases and two thresholds are shown in Fig. 10 for the one of 1.2 mm gap prototypes. It is seen from Fig. 10 that the use of the read-out pads on cathode side of RPC results in higher pads multiplicity.

All the previous data were obtained for the perpendicular incidence of the beam on the prototypes. In hadron calorimeters the active detectors should register particles in the wide range of the incidence angles. This item was studied using 1.6 mm gap prototype and 5% SF_6 mixture. The results are shown in Fig. 11. For the angles between beam direction and the normal to the prototype plane of 0^0; 30^0 and 45^0, no difference in efficiency and multiplicity dependence on applied voltage is seen.

4 Conclusion

As the first step in evaluating the possibility of using the RPCs operated in the saturated avalanche mode as an active detectors of the future DHCAL, several modifications of the monogap

RPC prototypes with the glass sheets as resistive electrodes were tested. Prototypes had 0.8; 1.2; 1.6 and 2.0 mm wide gas gaps and were equipped with (1×1) cm^2 readout pads.

The efficiencies of prototypes with gap width in the range 1.2–2.0 mm for the gas mixtures of TFE/isobutane/SF_6 containing 2 and 5% of SF_6 were measured to be above 98% for the threshold 2 mV corresponding to about 0.35 pC induced charge. The regions of the applied voltage in which the safe operation of the prototypes is ensured are wider for the 1.6 and 2.0 mm wide gas gaps than for the 1.2 mm one.

The charge characteristics of the prototypes were typical for the saturated avalanche mode of operation. In the whole operating regions the average charges do not exceed 6 pC with relatively low tails of large charges. The relative width of the charge distribution RMS_Q/Q_{mean} is lower for the wider gaps.

The fired pad multiplicity is of high importance when considering such RPCs as candidates for the active detectors of an imaging DHCAL. It was found that the mean multiplicity as low as at least 1.2 can be obtained by the proper RPC design.

It was found that the intrinsic noise rates of the RPCs in operating regions are higher for the more narrow gaps.

Prototypes characteristics do not change for the particle incidence angle up to 45^0.

As a result of this study some framework can be outlined for further RPC development.

– It seems appropriate to have FEE threshold of $\simeq$2 mV.

– From the electrical safety consideration lower voltage is preferable so the choice of the TFE/iC_4H_{10}/SF_6 = 93/5/2 gas mixture looks reasonable.

– The gas gap width between 1.2 and 1.6 mm should be choosen.

– The distance between the inner surface of the anode resistive electrode and the read-out plane should be made as short as possible.

The currently obtained characteristics of the 1.2 mm and 1.6 mm wide gap prototypes for 2% SF_6 fraction and 2.2 mV threshold are listed in the Table 1.

Table 1

No	Item	1.2 mm gap	1.6 mm gap
1	HV working point (200 V above knee), kV	8.4	9.0
2	HV plateau width for $\varepsilon \geq 98\%$, kV	0.55	1.0
3	Induced charge Q_{mean}, pC	3.5	3.0
4	RMS_Q/Q_{mean}	0.9	0.7
5	Pad multiplicity	1.45	1.45
6	Singles rate at plateau knee, Hz/cm^2	0.7	0.2

For the mixture containing 5% of SF_6 the required HV values are 0.8 (0.9) kV higher (Fig. 7a), while all other characteristics do not differ significantly from the ones presented above.

Acknowledgements

We wish to thank deeply A. Golovin for his hard work on manufacturing the RPC prototypes. The authors are grateful to CALICE Collaboration members especially to J-C.Brient, V.Korbel, J.Repond, F.Sefkow and H.Videau for valuable discussions and remarks.

This work was partially supported by the ECFA/DESY fund and by the RFBR grant No. 05-02-17037a.

References

1. TESLA Technical Design Report, part 4: A detector for TESLA, DESY 2001-011; ECFA 2001-209; TESLA report 2001-23; TESLA-FEL 2001-05, March 2001.
2. V.Ammosov, Nucl. Instr. Meth., vol. A494, 2002, 355.
3. V.Ammosov et al., Preprint DESY 04-057, Hamburg, 2004; Nucl. Instr. Meth., vol. A533, 2004, 130.
4. http://www.desy.de/conferences/ecfa-lc-study.html
5. http://polywww.in2p3.fr/flc/calor_LC.html
6. E.Usenko, IHEP preprint 2001-53, Protvino, 2001.

Received December 25, 2007.

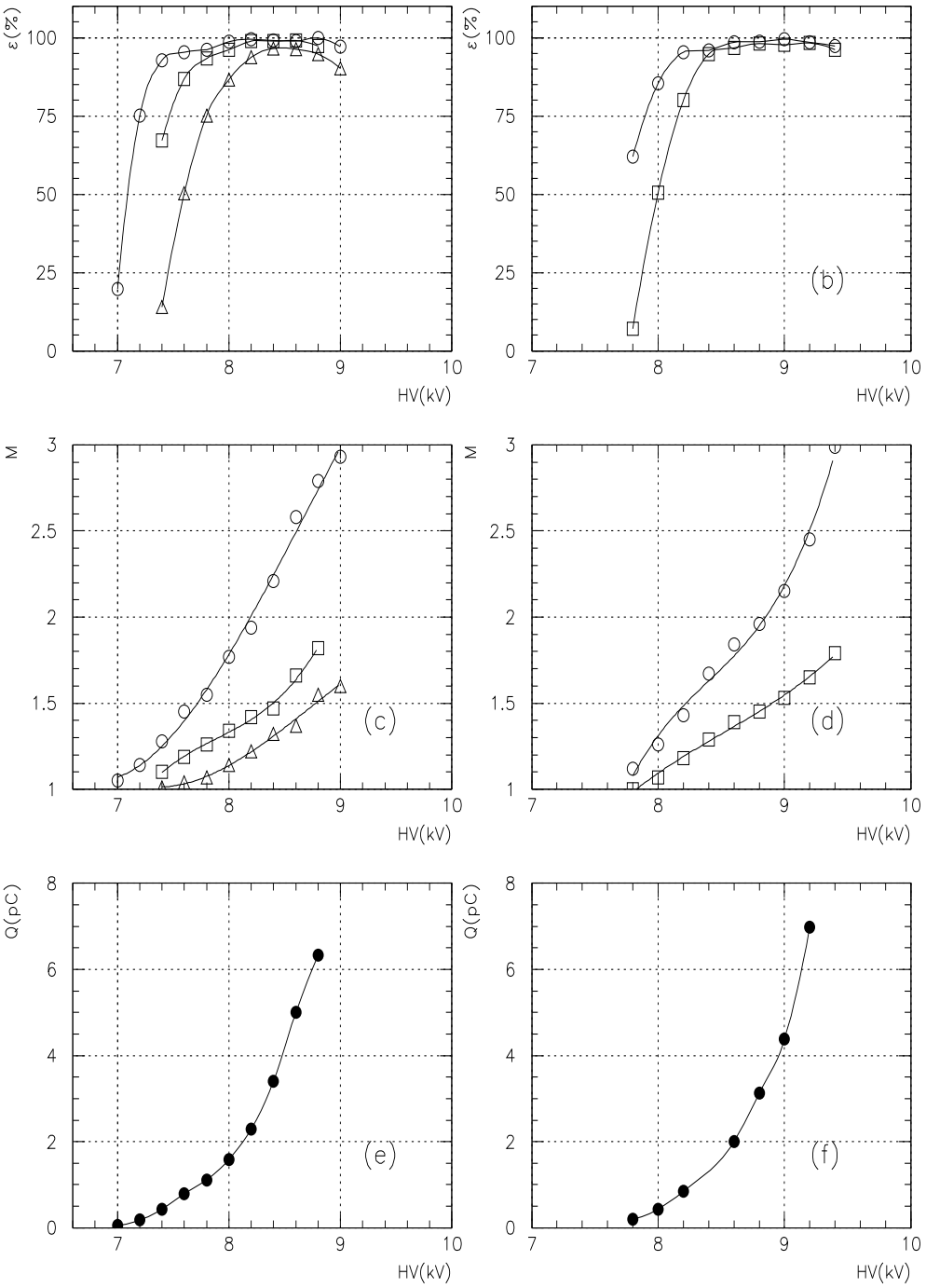

Figure 1. Efficiency (a, b), multiplicity (c, d) and mean charge (e, f) dependence on the HV for the 1.2 mm gap prototype. Left column — mixture with 2% of SF_6, right — 5%. Circles — threshold 0.6 mV, squares — 2.2 mV and triangles — 5 mV.

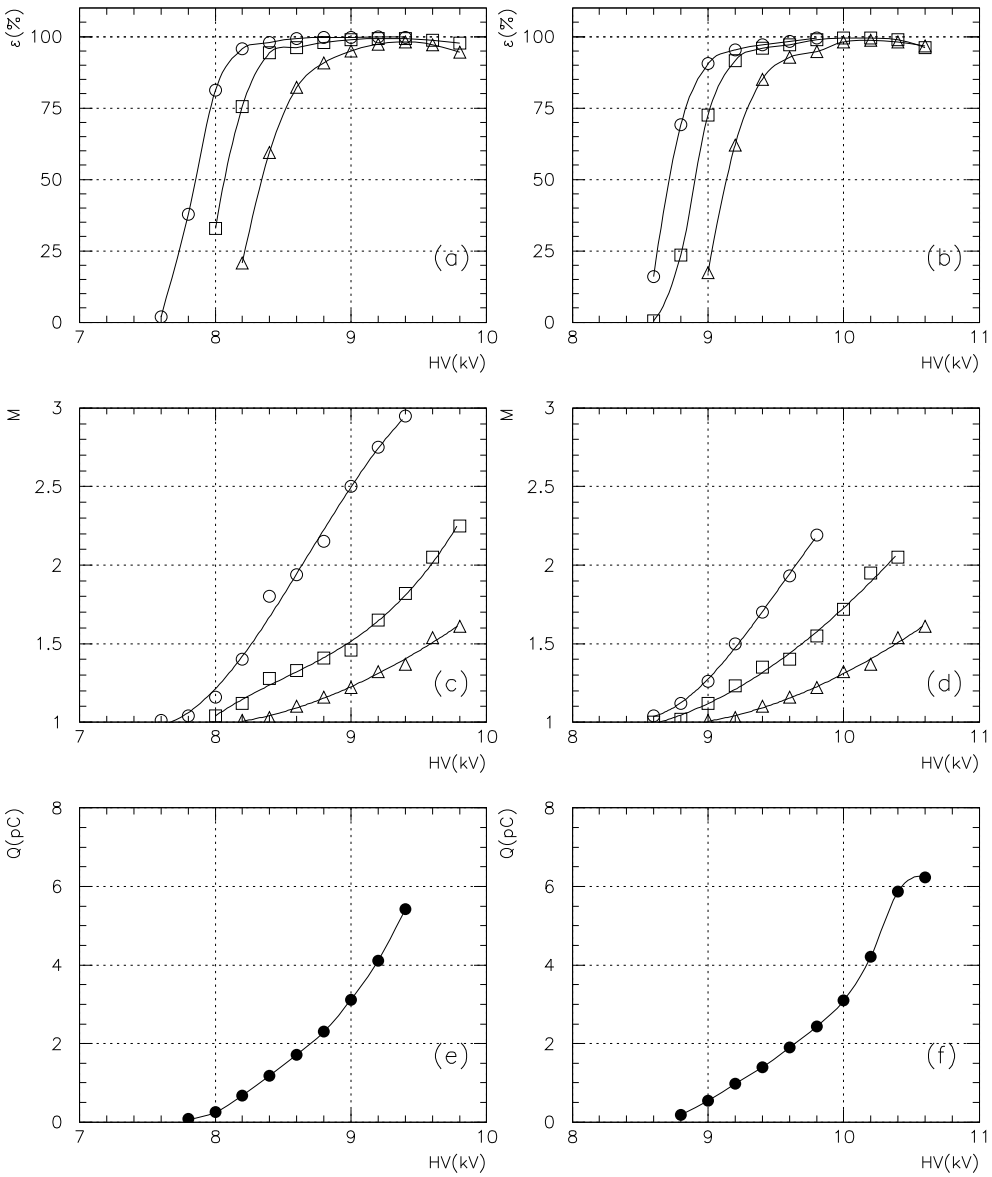

Figure 2. Efficiency (a, b), multiplicity (c, d) and mean charge (e, f) dependence on the HV for the 1.6 mm gap prototype. Left column — mixture with 2% of SF_6, right — 5%. Circles — threshold 0.6 mV, squares — 2.2 mV and triangles — 5 mV.

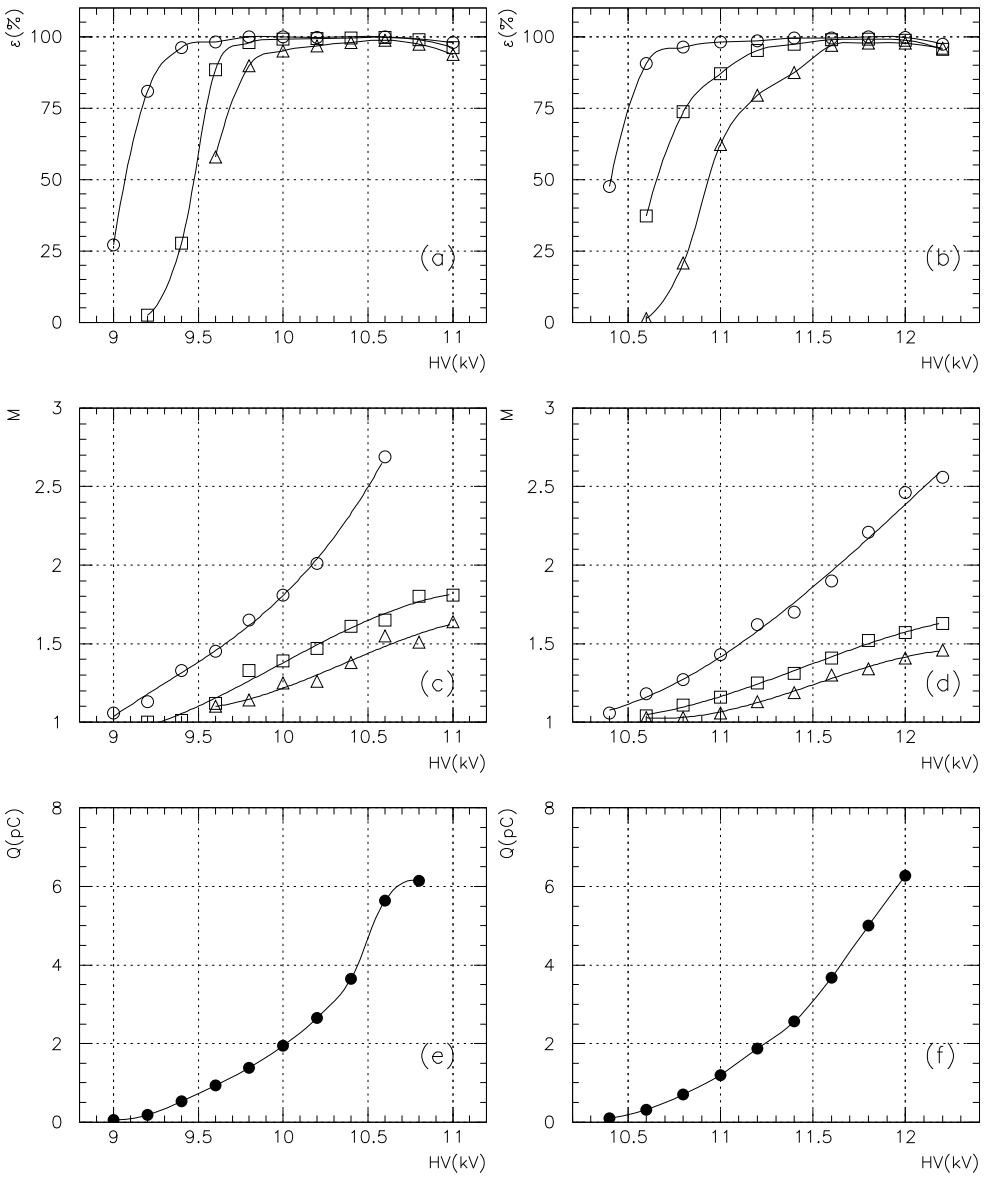

Figure 3. Efficiency (a, b), multiplicity (c, d) and mean charge (e, f) dependence on the HV for the 2.0 mm gap prototype. Left column — mixture with 2% of SF_6, right – 5%. Circles — threshold 0.6 mV, squares — 2.2 mV and triangles — 5 mV.

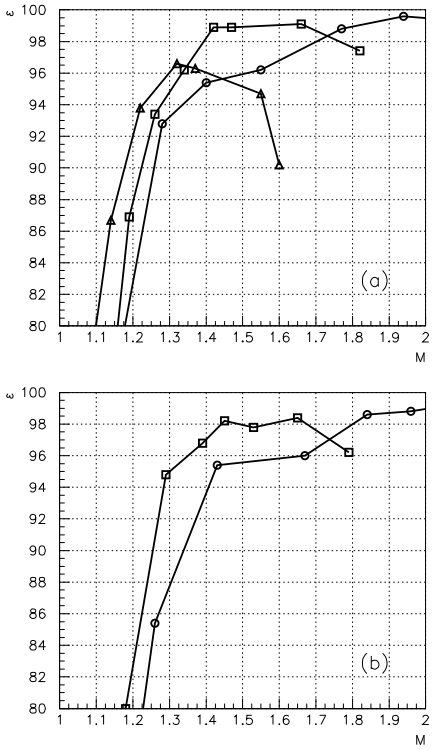

Figure 4. Correlation between efficiency ε and mean multiplicity M for prototype with 1.2 mm wide gap. (a) — mixture with 2% of SF_6, (b) — 5% SF_6. Circles — threshold 0.6 mV, squares — 2.2 mV, triangles — 5 mV.

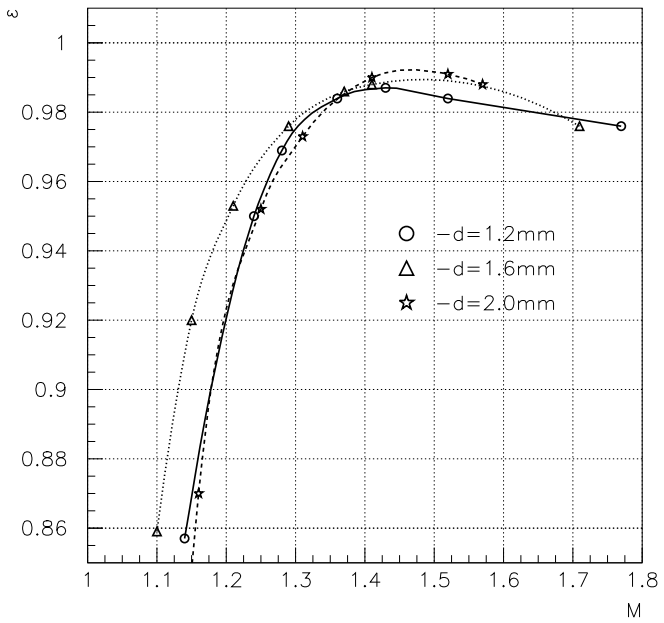

Figure 5. Correlation between efficiency ε and mean multiplicity M for prototypes with different gap width. Threshold is 2.2 mV.

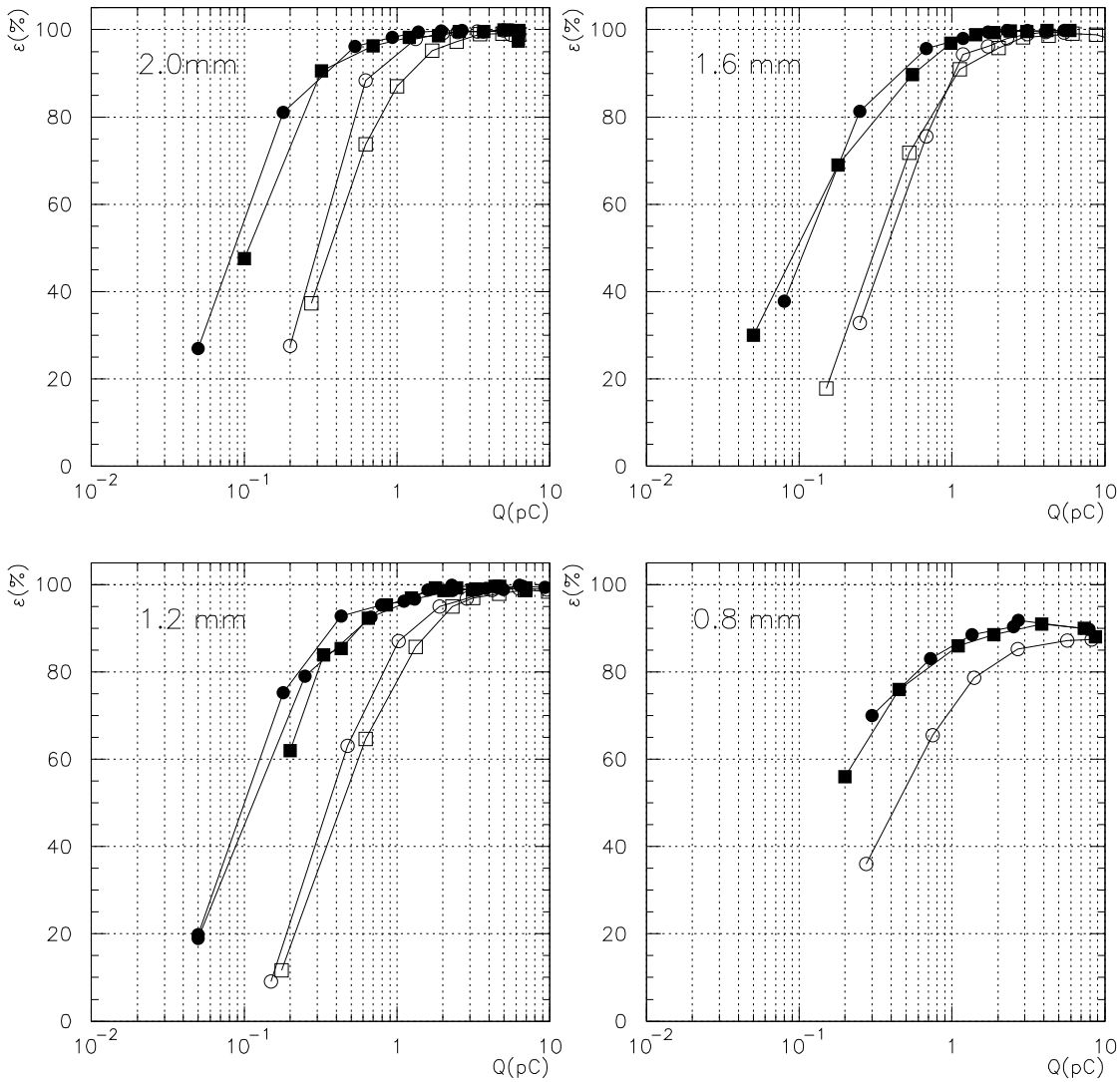

Figure 6. Efficiency ε dependence on the mean induced charge Q for prototypes with 2.0, 1.6, 1.2 and 0.8 mm wide gaps. Circles — mixture with 2% of SF_6, squares — 5%. Closed symbols — threshold 0.6 mV, open — 2.2 mV.

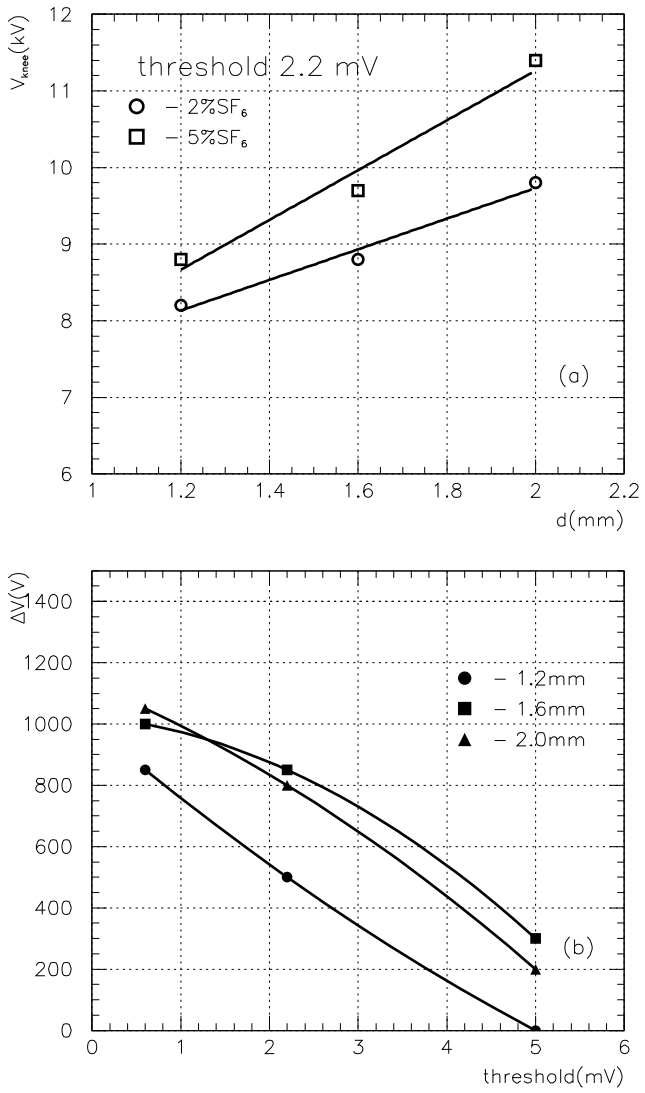

Figure 7. (a) — Applied voltage values for 98% efficiency V_{knee} for prototypes with different gap width d. (b) — Dependence of the operating region width ΔV on the threshold for three prototypes.

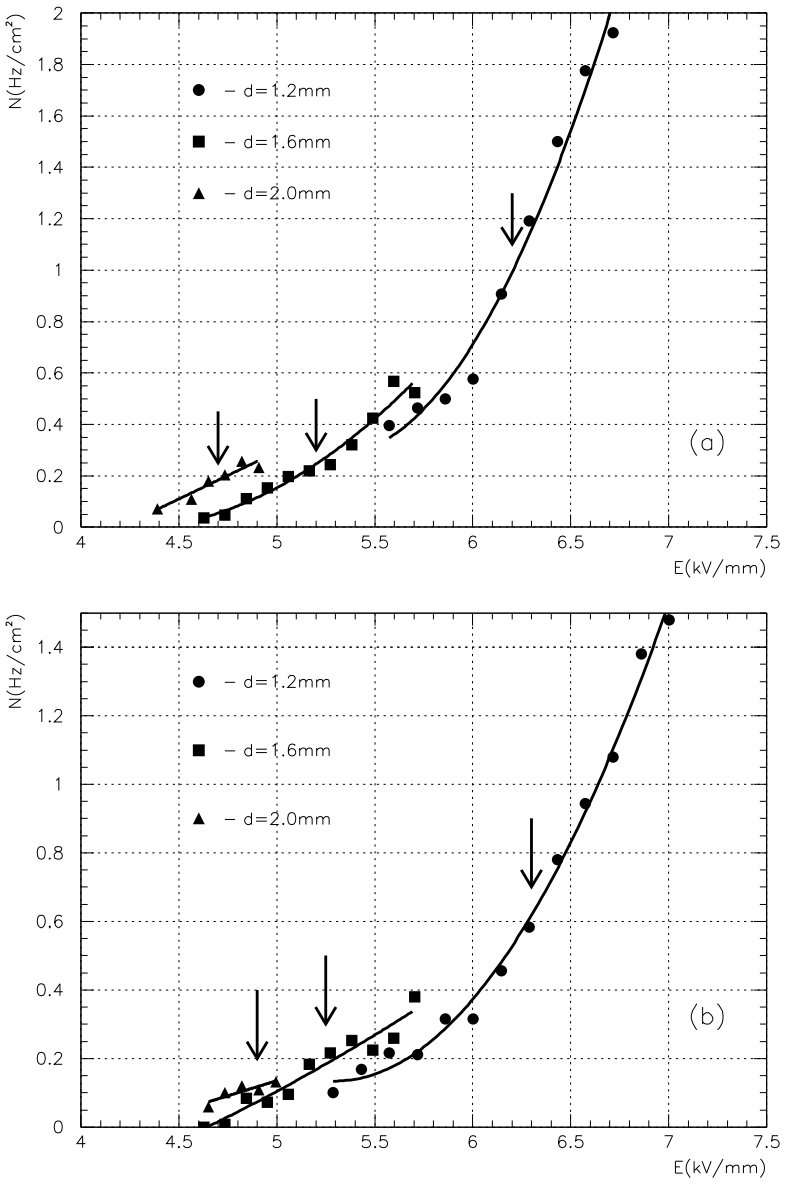

Figure 8. Noise rates N for prototypes with different gas gap width d in dependence on electrical field strength E, for 0.6 (a) and 2.2 (b) mV thresholds. Arrows depict knee values of E.

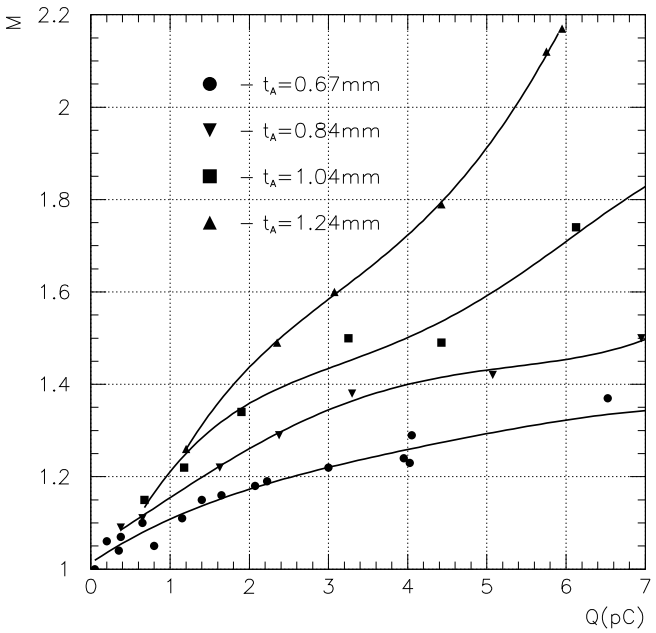

Figure 9. Mean multiplicity M dependence on induced charge Q for prototypes with different anode thickness t_A.

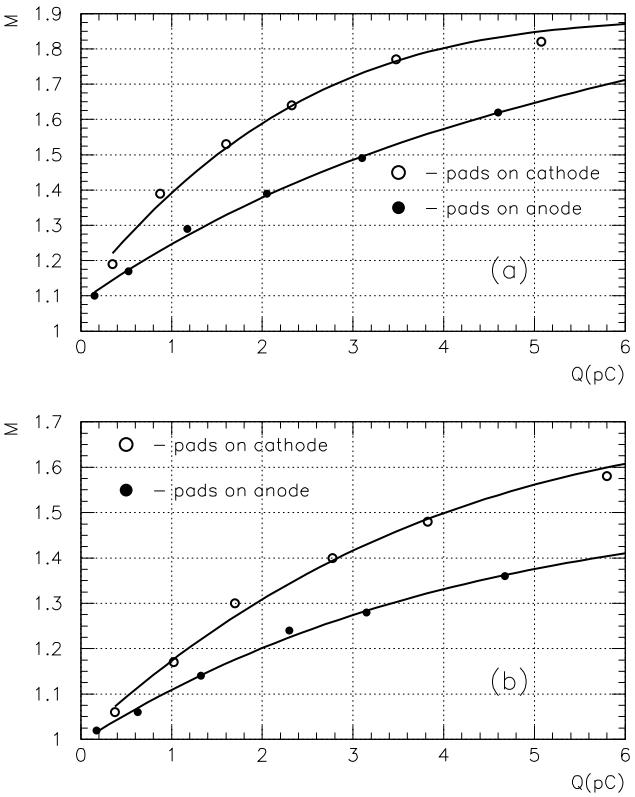

Figure 10. Mean multiplicity M dependence on induced charge Q for prototype with 1.2 gap width for two HV connection variants. (a) — threshold 0.6 mV, (b) — threshold 2.2 mV.

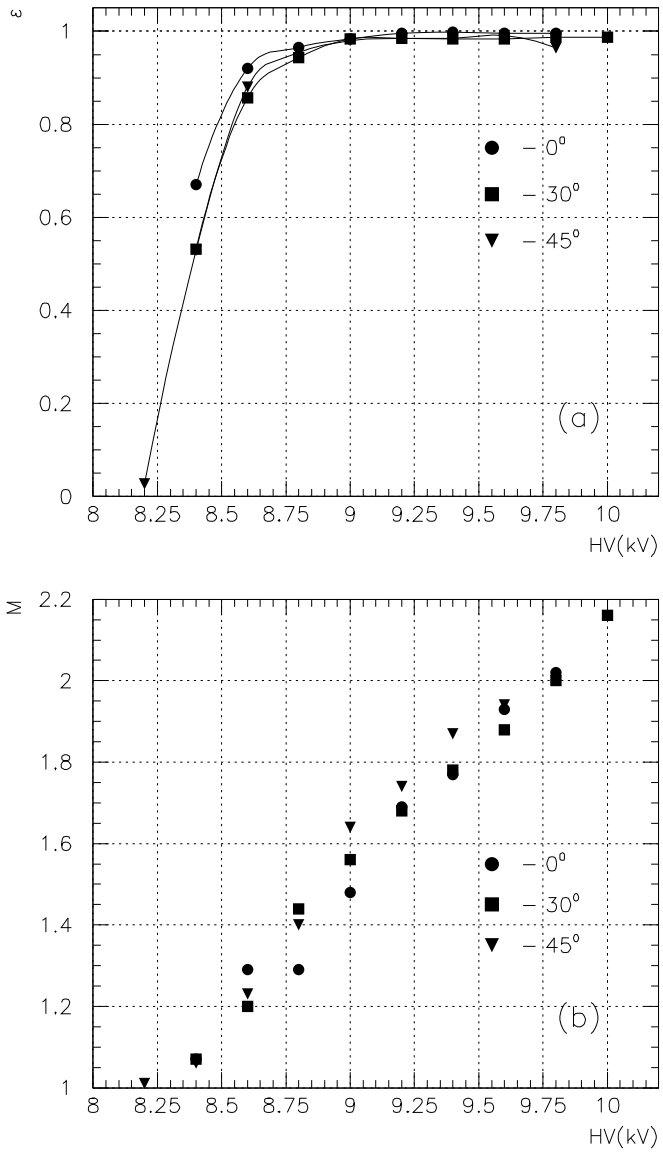

Figure 11. Efficiency (a) and mean multiplicity (b) dependence on applied voltage for different particle incidence angles.

Препринт отпечатан с оригинала-макета, подготовленного авторами.

В.В.Аммосов, В.А.Гапиенко, В.Г.Заец и др.
Изучение резистивных плоских камер с сигнальными элементами размером 1×1 см^2 в режиме насыщенной лавины.

Оригинал-макет подготовлен с помощью системы **LaTeX.**

Подписано к печати 26.12.2007. Формат $60 \times 84/8$.
Офсетная печать. Печ.л. 1,87. Уч.-изд.л. 1,7. Тираж 90. Заказ 130.
Индекс 3649.

ГНЦ РФ Институт физики высоких энергий
142281, Протвино Московской обл.

Индекс 3649

П Р Е П Р И Н Т 2007–22, И Ф В Э, 2007